Journal of The Electrochemical Society, **155** (9) J252-J255 (2008)
0013-4651/2008/155(9)/J252/4/$23.00 © The Electrochemical Society

A Study on the Luminescence Properties of $CaAlBO_4:RE^{3+}$ (RE = Ce, Tb, and Eu) Phosphors

Wei-Ren Liu,[a,z] Yi-Chen Chiu,[a] Chien-Yueh Tung,[a] Yao-Tsung Yeh,[a] Shyue-Ming Jang,[a] and Teng-Ming Chen[b,z]

[a]*Material and Chemical Research Laboratories, ITRI Hsichu 300, Taiwan*
[b]*Phosphors Research Laboratory and Department of Applied Chemistry, National Chiao Tung University, Hsinchu 30010, Taiwan*

A series of new phosphors of $CaAlBO_4:RE^{3+}$ (RE = Ce, Tb, Eu) were synthesized by conventional solid-state reactions. The X-ray diffraction data indicate that a pure phase of $CaAlBO_4:RE^{3+}$ can be successfully obtained. The photoluminescence (PL) spectra, quantum efficiency, and CIE coordinates of $CaAlBO_4:RE^{3+}$ were investigated. The PL and PL excitation spectra indicate that the emission wavelengths of $CaAlBO_4:Ce^{3+}$ are 372 and 398 nm (with full width at half maximum of 33 nm) attributed to the $4f^6 5d–4f^7$ transition of the Ce^{3+} activator, respectively. $CaAlBO_4:Tb^{3+}$ displays green emission at 483, 543, 584, and 620 nm, while $CaAlBO_4:Eu^{3+}$ shows a dominating emission peak at 621 nm, which is attributed to the Eu^{3+} $^5D_0 - {}^7F_2$ transition. The quantum efficiencies of optimized $CaAlBO_4:Ce^{3+}$, $CaAlBO_4:Tb^{3+}$, and $CaAlBO_4:Eu^{3+}$ were found to be 43, 21, and 19%, respectively. The phosphors may provide a new kind of luminescent material under UV excitation.
 [DOI: 10.1149/1.2953499]

Manuscript submitted March 5, 2008; revised manuscript received June 9, 2008. Published July 25, 2008.

Recently, great interest in phosphors has resulted in rapid developments in the promising display and illumination technologies. For general lighting, photoluminescent (PL) materials including oxides, silicates, aluminates, aluminoborates, aluminosilicates, nitrides, borates, etc., play very important roles for potential applications in UV light-emitting diodes. Among these hosts investigated, borates are good candidates as host structure due to their low synthetic temperature, easy preparation, and high luminescent brightness. The luminescence properties of UV-excitable Eu^{2+}-doped borate phosphors, such as $Ba_2LiB_5O_{10}$,[1] $Ba_2Mg(BO_3)_2$,[2] $Ba_2Ca(BO_3)_2$, $Sr_2Mg(BO_3)_2$,[3] $SrAl_2B_2O_7$,[4] $SrBPO_5$,[5] $Sr_2Al_2B_2O_8$,[6] and $M_2B_5O_9X$ (M = Ca, Sr; X = Cl, Br),[7] have been reported in the literature. Apart from Eu^{2+}-activated borates, several RE^{3+}-doped borates have also been studied, such as $BaAl_2B_2O_7$,[8] $(Y,Gd)BO_3$,[9] BaB_8O_{13},[10] and $CaAl_2B_2O_7$.[11,12] Recently, the luminescent properties of RE^{3+}-doped $CaYBO_4$ in the UV–vacuum UV spectral region have been reported by Wang and Wang[13] and Yang et al.,[14] where RE is Eu^{3+}, Tb^{3+}, Gd^{3+}, or Ce^{3+}. To the best of our knowledge, the luminescence properties of rare-earth-ion–activated $CaAlBO_4$ are not reported yet. The aim of this work is to report our investigation results on the synthesis, PL, and color chromaticity of the new indigo-blue ($CaAlBO_4:Ce^{3+}$), green ($CaAlBO_4:Tb^{3+}$), and red phosphors ($CaAlBO_4:Eu^{3+}$), and their corresponding spectroscopic properties under UV excitation.

Experimental

A series of $CaAlBO_4:RE^{3+}$ (RE = Ce, Tb, or Eu) phosphors were synthesized by solid-state reactions adopting $CaCO_3$ (99.99%, Aldrich), γ-Al_2O_3 (99.99%, Aldrich), B_2O_3 (>99.9%, Strem Chemicals), Eu_2O_3 (99.9%, Aldrich), Tb_4O_7 (99.9%, Strem Chemicals), and CeO_2 (99.998%, Strem Chemicals) as starting materials. The raw materials were weighed out in stoichiometric proportions and the mixtures were then fired at 1000°C for 10 h under N_2 atmosphere in an inner alumina crucible that was contained in a covered alumina crucible filled with graphite powder. The products were then obtained by cooling to room temperature in the furnace, ground, and pulverized for further measurements.

X-ray diffraction (XRD) was carried out on a Philips X'pert PRO diffractometer with Cu Kα (1.5418 Å) radiation. The PL and PL excitation (PLE) spectra were measured at room temperature by a Spex Fluorolog-3 spectrophotometer equipped with a 450 W Xe light source. All the spectra were measured with a scan rate of 150 nm min^{-1}. The CIE chromaticity coordinates were measured by a Laiko DT-101 color analyzer equipped with a charge-coupled device detector (Laiko Co., Tokyo, Japan). The reflectance spectra of the samples were collected with a Hitachi 3010 double-beam UV-visible (UV-vis) spectrometer (Hitachi Co., Tokyo, Japan) equipped with a ϕ60 mm integrating sphere inner face coated with Spectralon [poly(tetrafluoroethylene)], and α-Al_2O_3 was used as a standard in the measurements. The quantum efficiency (QE) was measured by an integrating sphere whose inner face was coated with Spectralon equipped with a spectrofluorometer (Horiba Jobin-Yvon Fluorolog 3–22 Tau-3). The device is based upon a Labsphere optical Spectralon integrating sphere (diameter of 100 mm), which provides a reflectance >99% over a 400–1500 nm range (>95% within 250–2500 nm). The sphere accessories were made from Teflon (rod and sample holders) or Spectralon (baffle). The measurement procedures of QE are described as follows. First of all, the empty quartz cell is placed on the light incident route of the sphere, and the optimal excitation light source alone is detected. The integral area of the excitation light is labeled as L_e. For the second step, the measurement is the same with step one except the sample is placed inside the sphere but not on the light incident route. The integral area of the excitation light source is labeled as L_o, and that of emission region is labeled as E_o. The third step is similar to the second, except that the sample is now directly stricken by the excitation light source. The integral area of the excitation light source is labeled as L_i, and that of the emission region is labeled as E_i.

Results and Discussion

The crystal structure of $CaAlBO_4$ was first reported by Schafer.[15] The Ca^{2+} ion in the lattice can be considered to be solely six-coordinated with Ca–O distance of 2.4053 Å. The JCPDS card no. 19–0204 reported the crystal structure is orthorhombic (space group Ccc2) with lattice constants a = 8.269 Å, b = 15.227 Å, and c = 5.733 Å. The XRD patterns of $CaAlBO_4$ at different synthesizing temperatures are shown in Fig. 1. With reaction temperatures at 800 or 900°C for 10 h, the major phases in the mixture are $CaAl_4O_7$ and $Ca_2B_2O_5$, which are confirmed by JCPDS card no. 23–1037 and 89–6630, respectively. With the reaction temperature up to 1000°C, a pure phase of $CaAlBO_4$ can be obtained. It is known that the ionic radii (r) of Ca^{2+} (CN = 6), Al^{3+} (CN = 4), and B^{3+} (CN = 3) are 1.00, 0.39, and 0.01 Å, respectively.[16] As a result of the ionic radii of doping rare-earth elements of Ce^{3+} (CN = 6, r = 1.01 Å), Tb^{3+} (CN = 6, r = 0.923 Å), and Eu^{3+} (CN = 6, r = 0.947 Å), it is difficult for RE^{3+} to substitute Al^{3+} or B^{3+} in the $CaAlBO_4$. Hence, in this study, it is believed that the Ca^{2+} sites are replaced by Ce^{3+}, Tb^{3+}, or Eu^{3+} in the lattice.

[z] E-mail: WRLiu@itri.org.tw; tmchen@mail.nctu.edu.tw

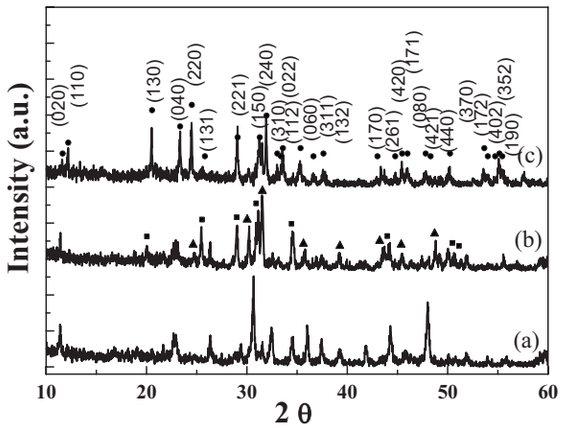

Figure 1. XRD pattern of $CaAlBO_4$ synthesized at different reaction temperatures for 10 h: (a) 800; (b) 900, and (c) 1000°C. (●) JCPDS card no. 19–0204 $CaAlBO_4$; (■) JCPDS card no. 23–1037 $CaAl_4O_7$, and (▲) JCPDS card no. 89–6630 $Ca_2B_2O_5$.

Figure 2 shows the reflectance spectra of pure $CaAlBO_4$ and RE^{3+} (RE = 0.1 mol % Ce^{3+}, 10 mol % Tb^{3+}, or 7 mol % Eu^{3+})-activated $CaAlBO_4$. The spectrum of pristine $CaAlBO_4$ exhibited the host absorption edge at ~330 nm from which the optical bandgap was estimated to be ~3.98 eV. The Ce^{3+}-doped $CaAlBO_4$ shows a broad hump at ~360 nm and a weak absorption band at around 330 nm. The former is due to host absorption and the latter is attributed to the 4f–5d transition of Ce^{3+}. The observation of host absorption in $CaAlBO_4$:Ce^{3+} mainly results from lower doping content of Ce^{3+} in the host and weaker luminescent intensity. The $CaAlBO_4$:Tb^{3+} shows a weak peak located at ~380 nm, which is due to f–f transition of Tb^{3+}, whereas Eu^{3+}-doped $CaAlBO_4$ displays an absorption peak at ~394 nm, which is typically ascribed to the f–f transition of Eu^{3+}. These results indicate that the emissions of Ce^{3+}, Tb^{3+}, and Eu^{3+} doped in $CaAlBO_4$ host correspond to the absorption of activators themselves.

We also investigated the optimization of luminescence performance of $CaAlBO_4$:RE^{3+} by tuning the respective dopant content, and Fig. 3 displays the PL intensity as a function of Ce^{3+}, Tb^{3+}, and Eu^{3+} dopant concentration for $(Ca_{1-x}Ce_x)AlBO_4$, $(Ca_{1-y}Tb_y)AlBO_4$, and $(Ca_{1-z}Eu_z)AlBO_4$, respectively. The optimal doping concentrations of Ce^{3+}, Tb^{3+}, and Eu^{3+} were found to be 0.1, 10, and 7 mol %, respectively. Beyond the critical concentration, the emission intensity begins to decrease due to concentration quenching of the activators. In order to further estimate the critical energy-transfer distance (R_c) between these activators in the host, the following equation[17] is valid because there is only one crystallographically distinct Ca^{2+} site with octahedral coordination in the $CaAlBO_4$ lattice. As a result, the critical energy-transfer distances between RE^{3+} ions for Eu^{3+}, Tb^{3+}, and Ce^{3+} in the three phosphors can be calculated by the following equation

$$R_c = 2\left(\frac{3V}{4\pi x_c N}\right)^{1/3} \quad [1]$$

where x_c is the critical concentration, N is the number of cation sites in the unit cell, and V is the volume of unit cell. In this case, V = 721.71 Å^3, N = 4, and the critical doping concentrations of Ce^{3+}, Tb^{3+}, and Eu^{3+} in $CaAlBO_4$ host were found to be 0.001, 0.1, and 0.07, respectively. Therefore, R_c of Ce^{3+}, Tb^{3+}, and Eu^{3+} were then determined to be 70.11, 15.10, and 17.01 Å, respectively, which were found to be in the range of those (i.e., ~35 and 20 Å) reported by Chang and Chen[18] and Xie et al.,[19] except for the Ce^{3+} activator. The larger value of R_c for Ce^{3+} may be due to the solubility of Ce^{3+} in $CaAlBO_4$ host. Compared to Tb^{3+} and Eu^{3+}, the ionic radius of Ce^{3+} is the largest, which causes the distortion of lattice while the doping content increases. The XRD patterns of $CaAlBO_4$:Ce^{3+} (not shown) with higher doping ratio reveals impurity phase of $Ca_2B_2O_5$ as long as the concentration of Ce^{3+} exceeds 1 mol %. The results of XRD patterns for $CaAlBO_4$:Tb^{3+} and $CaAlBO_4$:Eu^{3+}, however, are still pure phase, even when the doping content is up to 10 mol %.

In order to further determine the absolute QE of photoconversion for these phosphors, herein we have used the integrated sphere method for the measurements of optical absorbance (A) and quantum efficiency (Φ) of phosphor samples. The absorbance and quantum efficiencies of $CaAlBO_4$:RE^{3+} phosphors can also be calculated by using the following equations

$$A = \frac{L_0(\lambda) - L_i(\lambda)}{L_0(\lambda)} \quad [2]$$

where $L_0(\lambda)$ is the integrated excitation profile when the sample is diffusely illuminated by the integrated sphere's surface, and $L_i(\lambda)$ is the integrated excitation profile when the sample is directly excited by the incident beam. Furthermore, QE (Φ) of $CaAlBO_4$:RE^{3+} phosphors can be calculated by

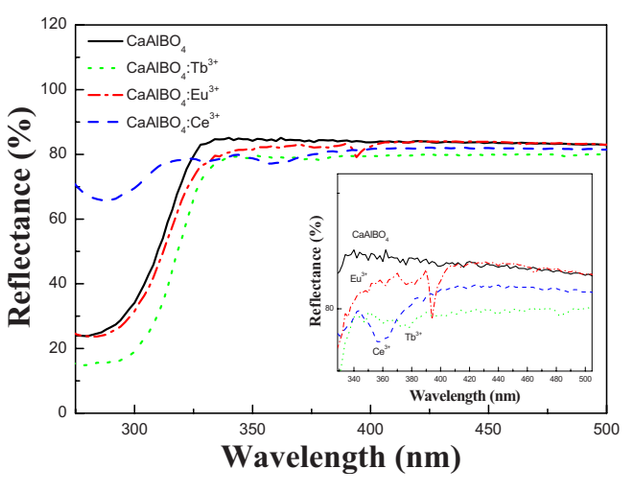

Figure 2. (Color online) Comparison of UV-vis diffuse reflectance spectra of $CaAlBO_4$ and as-synthesized $CaAlBO_4$:0.1% Ce^{3+}, $CaAlBO_4$:10% Tb^{3+}, and $CaAlBO_4$:7% Eu^{3+} phosphors. The inset illustrates reflection spectra of these phosphors by a larger magnitude.

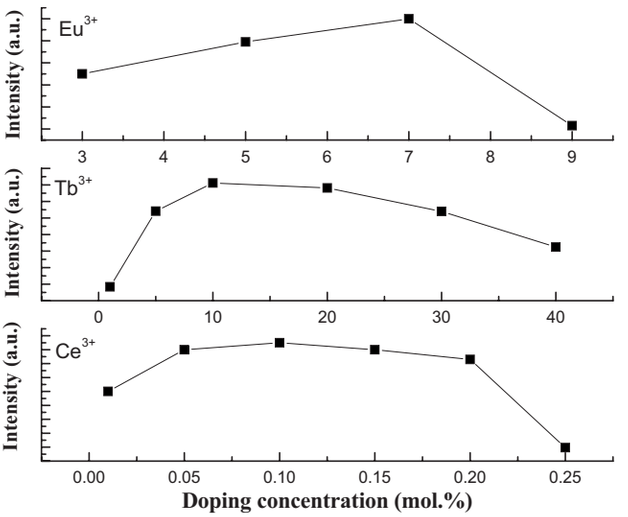

Figure 3. Emission intensity of $Ca_{1-x}AlBO_4$:xCe^{3+}, $Ca_{1-x}AlBO_4$:xTb^{3+}, and $Ca_{1-x}AlBO_4$:xEu^{3+} as a function of dopant concentration.

Table I. The comparison of commodity phosphors and $CaAlBO_4:RE^{3+}$ (RE = Ce, Tb, Eu).

Composition	Excitation (nm)	Emission (nm)	CIE (x, y)	Relative Absorbance	Relative QE
$BaMgAl_{10}O_{17}:Eu^{2+}$	343	452	(0.14, 0.07)	100	100
$CaAlBO_4$:0.1% Ce^{3+}	343	400	(0.16, 0.04)	60	45
$LaPO_4:Ce^{3+}$, Tb^{3+}	351	543	(0.30, 0.54)	100	100
$CaAlBO_4$:10% Tb^{3+}	351	543	(0.36, 0.50)	147	68
$La_2O_2S:Eu^{3+}$	393	621	(0.66, 0.33)	100	100
$CaAlBO_4$:7% Eu^{3+}	396	621	(0.54, 0.31)	74	90

$$\Phi = \frac{E_i(\lambda) - (1 - A)E_0(\lambda)}{L_e(\lambda)A} \quad [3]$$

where $E_i(\lambda)$ is the integrated luminescence of the powder upon direct excitation, and $E_0(\lambda)$ is the integrated luminescence of the powder excited by indirect illumination from the sphere. The term $L_e(\lambda)$ is the integrated excitation profile obtained from the empty integrated sphere (without the sample present). The absorbance of composition-optimized $CaAlBO_4:Ce^{3+}$, $CaAlBO_4:Tb^{3+}$, and $CaAlBO_4:Eu^{3+}$ were found to be 50, 29, and 38 at excitation wavelengths of 343, 351, and 396 nm, respectively, and the corresponding QE was found to be 43, 21, and 19%. For comparison, the values of A and QE of commodity phosphors $BaMgAl_{10}O_{19}:Eu^{2+}$ (blue), $LaPO_4:Ce^{3+}$, Tb^{3+} (green), and $La_2O_2S:Eu^{3+}$ (red) were also measured with the same approach. The corresponding excitation wavelengths, emission wavelengths, CIE coordinates, absorbance, and QEs are summarized in Table I. We have observed that the QE value of $CaAlBO_4:Eu^{3+}$ is close to that of the commodity $La_2O_2S:Eu^{3+}$ (Kasei-681).

Figure 4 shows the PL and PLE spectra of $(Ca_{0.999}Ce_{0.001})AlBO_4$, in which two excitation humps at 263 and 343 nm were observed in the PLE spectrum. The former is attributed to host absorption that was found to be consistent with the reflectance spectrum of pure $CaAlBO_4$ (Fig. 2). By Gaussian fitting, a stronger hump between 300 and 360 nm was observed to correspond to the 4f–5d transition of Ce^{3+}. The PL spectrum can be further deconvoluted by assuming a Gaussian-type profile into two emission peaks at 372 and 398 nm, attributed to the transition of 5d to $^2F_{5/2}$ and $^2F_{2/7}$, respectively. The energy difference between 372 and 398 nm is $\sim$1756 cm^{-1}, which is close to the theoretical value of $\sim$2000 cm^{-1}.[20] The Stokes shift for Ce^{3+} in $CaAlBO_4$ host is $\sim$4000 cm^{-1}, which was found to be located in the range of Stokes shift reported by Blasse and Bril for various Ce^{3+}-activated materials[21] (i.e., from 1200 cm^{-1} for $ScBO_3:Ce^{3+}$ and from 8000 cm^{-1} for $SrY_2O_4:Ce^{3+}$).

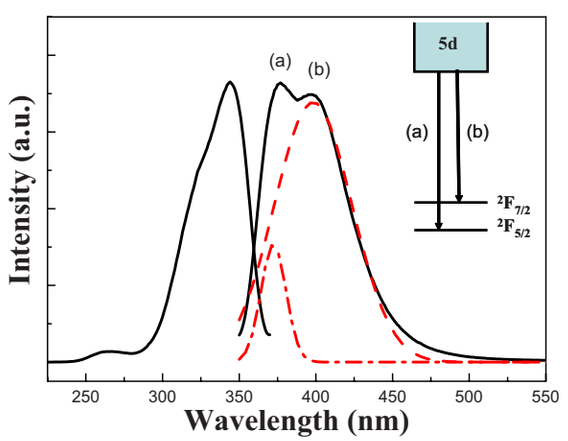

Figure 4. (Color online) Excitation and emission spectra of synthesized $CaAlBO_4$:0.1% Ce^{3+} phosphor.

Figure 5 displays the PL and PLE spectra of $(Ca_{0.9}Tb_{0.1})AlBO_4$ phosphor. The PLE spectrum shows sharp emission lines at 272, 284, 303, 317, 326, 341, 351, 354, 369, 374, and 379 nm, among which the excitation bands observed in the range of 230–300 nm are attributed to the $4f^8 \rightarrow 4f^75d^1$ transition of Tb^{3+}, and those in the range of 300–400 nm are due to the 4f $\rightarrow$ 4f transition of Tb^{3+}. The PL spectrum on the right side demonstrates typical Tb^{3+} emission due to the $^5D_4 \rightarrow {}^7F_J$ (J = 6, 5, 4, 3), which are $^5D_4 \rightarrow {}^7F_6$ (483, 490, 493 nm), $^5D_4 \rightarrow {}^7F_5$ (543, 555 nm), $^5D_4 \rightarrow {}^7F_4$ (585, 590 nm), and $^5D_4 \rightarrow {}^7F_3$ (621, 627 nm), respectively. The dominated green emission peak for $CaAlBO_4:Tb^{3+}$ is at 543 nm.

Figure 6 shows the PL and PLE spectra of composition-optimized $(Ca_{0.93}Eu_{0.07})AlBO_4$ phosphor. The broad-band at $\sim$260 nm can be attributed to the charge-transfer transition of $O^{2-} \rightarrow Eu^{3+}$, and the sharp lines between 300 and 420 nm were due

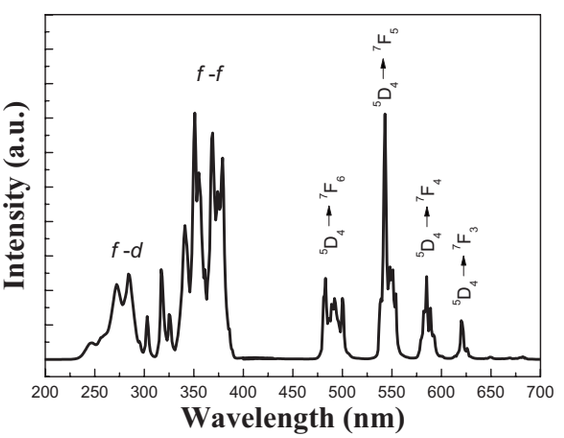

Figure 5. Excitation and emission spectra of synthesized $CaAlBO_4$:10% Tb^{3+} phosphor.

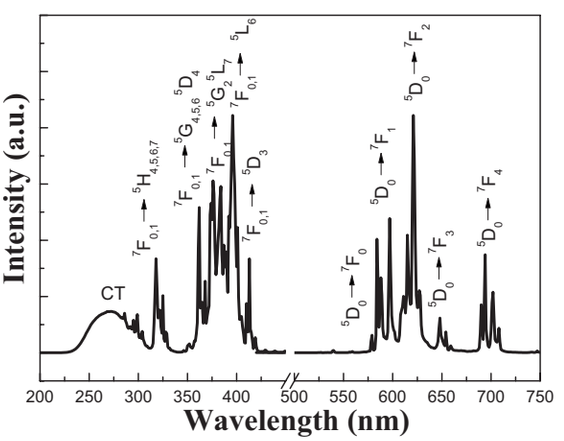

Figure 6. Excitation and emission spectra of synthesized $CaAlBO_4$:7% Eu^{3+} phosphor.

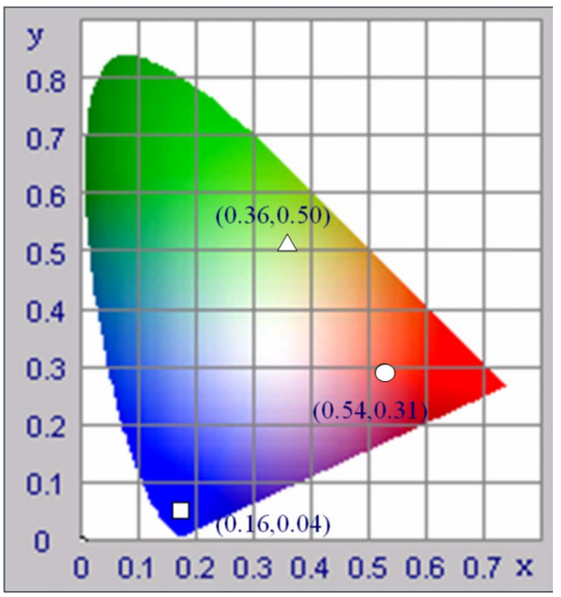

Figure 7. (Color online) CIE coordinates of $CaAlBO_4:Ce^{3+}$ (□), $CaAlBO_4:Tb^{3+}$ (△), and $CaAlBO_4:Eu^{3+}$ (○) phosphors, which are (0.16, 0.04), (0.36, 0.50), and (0.54, 0.31), respectively. The photos are taken under excitation at 365 nm in the UV box.

to the f–f transition of Eu^{3+} ions. The PL spectrum exhibited typical line emission assigned to the transition of $^5D_0$ to ^7F_J (J = 1, 2, 3, 4). It is well known that the highly intense line at 590 nm is due to magnetic dipole $^5D_0 \rightarrow {}^7F_1$ transition and the strong line at 621 nm is associated with the electric dipole transition. In this study, the dominant emission peaks of $CaAlBO_4:Eu^{3+}$ located at 621 nm are due to electric dipole transition, indicating that Eu^{3+} ion occupied the site of noninversion symmetry.[22] The emission peak of Eu^{3+} at ~579 nm originating from the $^5D_0 \rightarrow {}^7F_0$ transition is a forbidden transition. The $^5D_0 \rightarrow {}^7F_0$ transition is observed when Eu^{3+} occupies a lattice site with C_v, C_{nv}, or C_s symmetry. In this study, a single emission peak at 579 nm indicates that Eu^{3+} solely occupied one Ca^{2+} cite, and this observation is consistent with site symmetry of Ca^{2+} and the crystal structure of $CaAlBO_4$.

Figure 7 shows the CIE chromaticity diagram with empirically measured CIE coordinates under excitation of 365 nm. The chromaticity coordinates of optimized phosphors, $(Ca_{0.999}Ce_{0.001})AlBO_4$, $(Ca_{0.9}Tb_{0.1})AlBO_4$, and $(Ca_{0.93}Eu_{0.07})AlBO_4$, were found to be (0.16, 0.04), (0.36, 0.50), and (0.54, 0.31), respectively. The diagram shown in Fig. 7 displays indigo-blue, green, and red color under 365 nm excitation, which indicates that $CaAlBO_4:RE^{3+}$ (RE = Ce, Tb, Eu) are good candidates as indigo-blue, green, and red luminescence materials for application under UV excitation.

Conclusions

In summary, new phosphors of $CaAlBO_4:RE^{3+}$ (RE = Ce, Tb, Eu) that emit indigo-blue, green, and red lights have been reported and the dominant emission wavelengths were found to be 398, 543, and 620 nm under optimal excitation wavelengths at 343, 351, and 393 nm, respectively. The optimized doping contents of Ce^{3+}, Tb^{3+}, and Eu^{3+} in $CaAlBO_4$ were determined to be 0.1, 10, and 7 mol %, respectively. The experimental QE data have indicated that these phosphors may be potential candidates for applications in luminescent materials under UV excitation.

Acknowledgment

The authors acknowledge generous financial support from Industrial Technology Research Institute.

Industrial Technology Research Institute assisted in meeting the publication costs of this article.

References

1. G. J. Dirksen and G. Blasse, *J. Solid State Chem.*, **92**, 591 (1991).
2. A. Akella and D. A. Keszler, *Mater. Res. Bull.*, **30**, 105 (1995).
3. A. Diaz and D. A. Keszler, *Chem. Mater.*, **9**, 2071 (1997).
4. F. Lucas, S. Jaulmes, and M. Quarton, *J. Solid State Chem.*, **150**, 404 (2000).
5. K. Sakasai, M. Katagiri, K. Toh, N. Takahashi, M. Nakazawa, and Y. Kondo, *J. Appl. Phys.*, **74**, S1589 (2002).
6. M. Schläger and R. Hoppe, *Z. Anorg. Allg. Chem.*, **619**, 976 (1993).
7. M. J. Knitel, B. Hommels, P. Dorenbos, C. W. E. Van Eijk, I. Berezovskaya, and V. Dotsenko, *Nucl. Instrum. Methods Phys. Res. A*, **449**, 595 (2000).
8. T. R. N. Kutty, R. Jagannathan, and R. P. Rao, *Mater. Res. Bull.*, **25**, 343 (1990).
9. Y. Wang, K. X. Guo, T. Endo, Y. Murakami, and M. Ushirozawa, *J. Solid State Chem.*, **177**, 2242 (2004).
10. Q. Zeng, Z. Pei, and Q. Su, *J. Lumin.*, **82**, 241 (1999).
11. H. You and G. Hong, *Mater. Res. Bull.*, **32**, 785 (1997).
12. H. Yang, C. Li, H. He, G. Zhang, Z. Qi, and Q. Su, *J. Lumin.*, **124**, 235 (2007).
13. L. Wang and Y. Wang, *J. Lumin.*, **126**, 160 (2007).
14. H. Yang, C. Li, Y. Tao, J. Xu, G. Zhang, and Q. Su, *J. Lumin.*, **126**, 196 (2007).
15. K. Schafer, *Neues Jahrb. Miner. Monatsh.*, **1967**, 131.
16. R. D. Shannon, *Acta Crystallogr. A*, **32**, 751 (1976).
17. G. Blasse, *J. Solid State Chem.*, **62**, 207 (1986).
18. C.-K. Chang and T.-M. Chen, *Appl. Phys. Lett.*, **91**, 081902 (2007).
19. R.-J. Xie, N. Hirosaki, Y. Yamamoto, T. Suehiro, M. Mitomo, and K. Sakuma, *J. Ceram. Soc. Jpn.*, **113**, 462 (2005).
20. G. Blasse and B. C. Grabmaier, *Luminescent Materials*, p. 45, Springer, Berlin (1994).
21. G. Blasse and A. Bril, *J. Chem. Phys.*, **47**, 5139 (1967).
22. G. Blasse, *Chem. Phys. Lett.*, **20**, 573 (1973).